

Resonances of Energetic Particle Instabilities

During Frequency Chirping*

D.C. Pace¹, W.W. Heidbrink², M.A. Van Zeeland¹

¹ General Atomics, P.O. Box 85608, San Diego, CA 92186-5608, USA

² University of California Irvine, University Dr., Irvine, CA 92697, USA

Convective energetic ion transport results from Alfvén eigenmodes (AEs) and energetic particle modes (EPMs) due to resonances between these modes and the orbit topology of the ions. Experiments at the DIII-D tokamak [1] show that ion/EPM resonance space can be selectively probed as limited resonances produce energetic ion losses that are coherent at the mode frequency. A particular set of modes are the focus of the present work: these modes exhibit fast frequency chirping and represent a highly nonlinear interaction with beam ions. This phenomena is especially sensitive to details of the energetic ion phase space, therefore making it an incredibly useful scenario for validating models of energetic ion transport due to MHD. A simplified analysis readily identifies these resonances using experimental quantities, and these results are applied to the development of future experiments.

Neutral beam injection in the DIII-D tokamak ($R = 1.7$ m, $a = 0.6$ m) occasionally results ($\approx 3\%$ of discharges) in the excitation of energetic ion modes characterized by a fast downward frequency chirp as shown in the density spectrogram of Fig. 1. These modes evolve in frequency much faster than the equilibrium (i.e., much faster than the more standard frequency evolution of a reversed shear Alfvén eigenmode), often chirping through $\Delta f = 20$ kHz in approximately 1 ms.

Resonances between AEs and energetic ions (beam ions in these DIII-D experiments) are identified when the following resonance condition is met,

$$\omega + (m+l)\omega_\theta - n\omega_\zeta = 0 \quad (1)$$

where ω is the mode frequency, m is the poloidal mode number, l is an integer quantum number, ω_θ is the ion poloidal transit frequency, n is the toroidal mode number, and ω_ζ is the ion toroidal transit frequency. The ion orbit frequencies are calculated by a constants of motion code that calculates gyrocenter trajectories [2]. The code identifies values of $p = m+l$ that

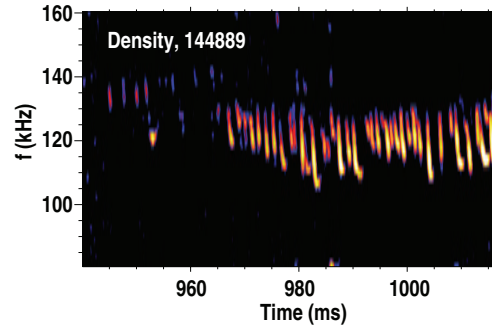


Figure 1: Cross-power spectrum from two channels of the interferometer diagnostic indicating density fluctuations that exhibit frequency chirping.

satisfy the resonance condition through $p = (\omega - n\omega_\zeta)/\omega_\theta$. In this application, the value of the poloidal mode number is set as $m = nq_{\text{mode}}$, where q_{mode} is the value of q at the mode location. The actual functional dependence, $m = m(n, q_{\text{mode}})$, depends on the mode frequency, e.g., for a TAE with $\omega = v_A/(2qR)$ we have $m = nq_{\text{mode}} - 1/2$. The approximation $m = nq_{\text{mode}}$ is sufficient because a range of p -values are searched for resonances. Even if the value of m is incorrect for a particular mode, the resonances will still be identified based on the wide range of p that is searched (a range determined by the user-provided range of l -values). This allows for an efficient and relatively quick calculation of the resonance space that can help to explain experimental observations.

The efficiency of this analysis is the motivation for applying it to experiments. All of the quantities used in this consideration are readily measured in a tokamak experiment. Codes that identify resonances based on solving for complete mode eigenfunctions (e.g., HAGIS [3]), require considerably more input effort and computational resources (they will provide a more complete physics output, however). In balance, the simplified techniques discussed here provide immediate guidance concerning the ion-wave interactions, and ways to modify them, while not precluding the application of more comprehensive physics models in future analysis.

An example of the beam ion - AE resonance phase space is shown in Fig. 2 for a chirping observation. The color contours represent the initial energetic ion distribution resulting from beam deposition. Beam ion velocities for injection at $E_{\text{beam}} = 81$ keV are sub-Alfvénic for this plasma with $B_T = 1.9$ T and $\bar{n}_e = 2.1 \times 10^{19} \text{ m}^{-3}$, therefore the beam ion distribution is shown only for the full energy (the interaction between beam ions and AEs is largest for the ions with the greatest velocity). The phase space is plotted as a function of toroidal canonical momentum (P_ϕ) normalized to the poloidal magnetic flux at the separatrix (Ψ_{wall}), and the magnetic moment (μ) normalized to the central value (E/B). Concentrations of beam ion density result from the individual beam geometries. Overlaid on the beam ion distribution is a set of AE resonances calculated based on the measured properties of one of the chirping modes. The central frequency of the chirp range, 70 kHz, is used along with the toroidal mode number of $n = 3$. Coherent beam ion losses at 70 kHz are measured by the fast ion loss detector (FILD) [4] in this plasma, and the location of that obser-

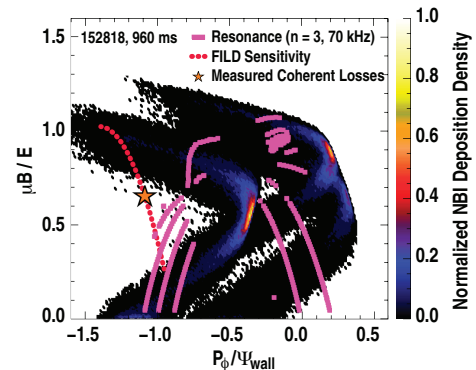


Figure 2: Beam ion deposition (color contours) along with resonances for the observed $n = 3, 70$ kHz Alfvénic chirping mode. The sensitivity (at $E_{\text{ion}} = 81$ keV) of the FILD is indicated by the dotted line, and the \star -symbol marks the observed coherent beam ion losses (i.e., occurring at 70 kHz).

vation is indicated by the \star -symbol along the dotted line representing the entire sensitivity of the FILD system. Since the FILD observations also involve ions at $E = 81$ keV, this analysis effectively maps the phase space transport of beam ions: the ions originate from the resonance-deposition overlap areas that are closest to the FILD measurement marker. A second FILD [5] does not measure any coherent losses from the chirping mode. This lack of observed losses is sensible considering that the sensitivity of the second FILD exists at values of $P_\phi/\Psi_{\text{wall}}$ that are more negative than the detector shown in Fig. 2, and therefore it exists too far away from the resonances (in phase space) to detect the interaction.

Considering the full energy beam ions as the primary source of interaction with the Alfvénic modes also allows for an assessment of the relative strength of the resonances. This is described by Fig. 3. Figure 3(a) shows a beam ion deposition distribution and resonance curves from a shot in which chirping modes were observed with $n = 1$ at a central frequency of 54.4 kHz. While a complete assessment of this situation requires acknowledging the actual beam ion slowing down distribution that occurs over time, it is reasonable to consider the full beam energy component as the complete energetic ion distribution for time periods shortly following the initial beam injection. The resonances from this shot are plotted in Fig. 3(b) according to the total number of beam ions with which they overlap.

The source of free energy for driving the modes is actually caused by gradients in phase space, and those traces are plotted in Fig. 3(c). The strongest resonant interaction is the one that passes nearly perfectly through the beam deposition curves resulting from the combined injection of tangential and perpendicular beam lines. This serves as an example of an area in which a more comprehensive code is ultimately needed; the energy transfer between the AE and ion depends on $\int_{\text{orbit}} \vec{v} \cdot \vec{E}$, where \vec{v} is the ion velocity, \vec{E} is the electric field of the AE, and the integral is taken over the trajectory of the ion [6]. The beam ion density gradient analysis of Fig. 3(c) does not account for the $\vec{v} \cdot \vec{E}$ term over the actual trajectory of the ion, therefore, this is not an accurate measure of the energy exchange.

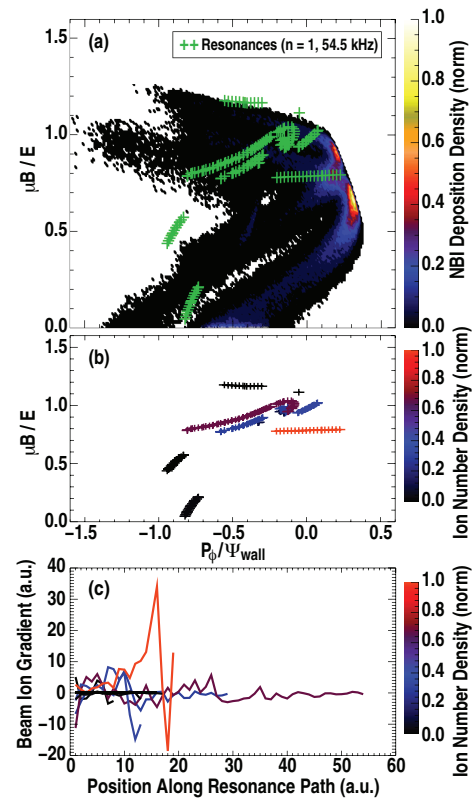


Figure 3: Shot 152818: (a) Beam ion deposition (color contour) along with resonances from a chirping Alfvén eigenmode (+-symbols). (b) Resonances paths from panel (a) plotted according to the number of beam ions with which they overlap. (c) Beam ion phase space gradient along the resonance paths.

Considering its range of applicability, a host of experimental ideas follow from this type of phase space analysis. The beam ion gradients corresponding to strongest resonant interaction identified in Fig. 3(c) can be manipulated through appropriate changes in plasma or beam parameters. For example, replacing the perpendicular beams with all tangential beams would allow for the same plasma parameters (i.e., the auxiliary heating power can be matched), while changing (likely reducing) the beam ion gradients in that area of phase space. Developing experiments that systematically probe beam ion distributions in this way is important for the mode validation effort since the applicability and confidence of such models, as they are applied to predictions for future fusion devices, is determined based on their ability to reproduce existing experiments.

In conclusion, a simplified analysis of resonances between Alfvén eigenmodes and beam ions is applied to DIII-D experiments featuring fast frequency chirping modes. Combining the measured AE characteristics with beam ion orbit frequencies allows for an efficient method of generating a toroidal momentum - magnetic moment phase space that readily identifies interactions that likely lead to convective beam ion loss. This information is used to identify adjustments in experimental parameters (e.g., beam duty cycles) that provide for improved systematic investigation of beam ion transport due to AEs and EPMS.

References

- [1] J.L. Luxon, *Nucl. Fusion* **42**, 614 (2002)
- [2] M.A. Van Zeeland, et al., *Phys. Plasmas* **18**, 056114 (2011)
- [3] S.D. Pinches, et al., *Comp. Phys. Comm.* **111**, 133 (1998)
- [4] X. Chen, et al., *Rev. Sci. Instrum.* **83**, 10D707 (2012)
- [5] R.K. Fisher, et al., *Rev. Sci. Instrum.* **81**, 10D307 (2010)
- [6] W.W. Heidbrink, *Phys. Plasmas* **15**, 055501 (2008)

*This work was supported by the US Department of Energy under DE-FC02-04ER54698 and SC-G903402.